Scaling Approach for Estimating Stand Sapwood Area from Leaf Area Index in Five Boreal species

M. Rebeca Quiñonez-Piñón and Caterina Valeo

September 2019

forests

MDPI

Article

Scaling Approach for Estimating Stand Sapwood Area from Leaf Area Index in Five Boreal species

M. Rebeca Quiñonez-Piñón [1] and Caterina Valeo [2,*]

[1] Geomatics Engineering, Schulich School of Engineering, University of Calgary, 2500 University Drive NW, Calgary, AB T2N 1N4, Canada; mrquinon@gmail.com

[2] Mechanical Engineering, University of Victoria, P.O. Box 1700 STN CSC, Victoria, BC V8W 2Y2, Canada

* Correspondence: valeo@uvic.ca; Tel.: +1-250-721-8623

Received: 29 July 2019; Accepted: 18 September 2019; Published: 20 September 2019

Abstract: This paper presents a scaling approach for estimating sapwood area at the stand level using knowledge obtained for individual trees of five boreal species: *Populus tremuloides* (Michx.), *Pinus contorta* (Doug. ex Loud. var. *latifolia* Engelm.), *Pinus banksiana* (Lamb.), *Picea mariana* (Mill.) BSP, and *Picea glauca* (Moench) Voss. Previously developed allometric models for sapwood depth and diameter at breast height for individual tree species were used to build stand level sapwood area estimates as well as stand level leaf area estimates, in pure and mixed vascular vegetation stands. A stand's vegetation heterogeneity is considered in the scaling approach by proposing regression models for each species. The new combined scaling approach drew strong linear correlations at the stand scale between sapwood area and leaf area using observations taken in mixed stands of Southern Alberta, Canada. This last outcome suggests a good linear relationship between stand sapwood area and stand leaf area. The accuracy of the results was tested by observing each regression model's adequacy and by estimating the error propagated through the whole scaling process.

Keywords: sapwood area; leaf area; boreal forest; scaling approaches; allometric correlations; error propagation; *Populus tremuloides*; *Pinus banksiana*; *Pinus contorta*; *Picea mariana*; *Picea glauca*

1. Introduction

Sapwood area supports several physiological functions, such as photosynthesis, gas ex-change, cooling, nutrient transport, and transpiration. Also, sapwood area has been theoretically related to leaf area with Shinozaki's pipe model theory [1]. The pipe model theory is supported by several studies, most of which modeled species specific leaf area (LA_{sp}) versus sapwood area (SA_{sp}) to estimate a single tree's leaf area (where the tree's sapwood area is the predictor). Linear models for about 20 conifers, such as Scots pine (*Pinus sylvestris* L.) [2]; Ponderosa pine (*Pinus ponderosa* Douglas ex Lawson) [3]; Loblolly pine (*Pinus taeda* L.) [4]; Douglas fir (*Pseudotsuga menziesii* (Mirbel) Franco) [3,5,6]; Lodgepole pine (*Pinus contorta*) [7–10]; Engelmann spruce and Subalpine fir (*Picea engelmanni* Parry ex Engelmann and *Abies lasiocarpa* (Hooker) Nuttall) [10]; Pinyon pine (*Pinus edulis* Engelmann) and One-seeded Juniper (*Juniperus monosperma* (Engelmann) Sargent) [11]; and Balsam fir (*Abies balsamea* (L.) Mill.) [12,13], were reported. While deciduous species haven't been studied as greatly as coniferous species, there are some published works for Mountain ash (*Eucalyptus regnans* F. Muell.) [14]; Trembling aspen (*Populus tremuloides*) [10]; and Cherry bark oak (*Quercus falcate* Q.Pagoda) and Green ash (*Fraxinus pensylvanica* Marshall) [15]. In this last work, the model for predicting leaf area was improved by not only having sapwood area as a predictor, but by adding total height and live crown ratio to the model [15].

Researchers studying the same species under different site conditions have reported different LA_{sp}:SA_{sp} regression models (linear and non-linear). The discrepancy between results have helped to

understand that the LA_{sp}:SA_{sp} relationship is driven by site conditions such as stand density [16–18], climatic factors [19], and physical characteristics [20]. Naturally, it is expected that the LA_{sp}:SA_{sp} relationship is species-specific [20], but this has not always been observed. For example, the Lodgepole pine (*Pinus contorta*) LA_{sp}:SA_{sp} allometric relationship is linear [21] but in another study, a nonlinear regression better explained this relationship [10]. Thus, while in theory the LA_{sp}:SA_{sp} relationship is positioned as linear, this could change due to site conditions.

Average sapwood depth ($\overline{sd}$) has been used instead of sapwood area to indirectly estimate other forest stand characteristics such as canopy cover densities and foliage biomass, by combining remotely sensed data and field data [22,23]. The method consists of estimating foliage biomass as a function of the diameter at the breast height *(D)* by previously modelling $\overline{sd}$:D relationships to predict D for a whole tree stand [23]. The authors used equations to estimate foliage biomass and sapwood area. A previously reported relationship for $\overline{sd}$:D to estimate foliage biomass was used as an indicator of D in [22]. The $\overline{sd}$:D relationship used in both studies was obtained from [24]. To the authors' knowledge, [24] is one of a very small number of published works reporting results for single tree $\overline{sd}$:D relationships ([24] cited three more published works on this topic). In Douglas fir (*Pseudotsuga menziesii*) and some other conifers, sapwood depth increases as the inside bark tree's diameter increases [24]. Most of the species showed that trees had an exponential sapwood depth growth until they reached a diameter of 25.4–38.1 cm, where sapwood depth would then plateau. Sapwood depth in older trees tended to increase at a slower rate than younger trees. Except for *Pinus contorta*, this was the general tendency, where there was large variability in sapwood depth, and some trees that were smaller in diameter showed a larger sapwood depth than those with a larger diameter. Douglas fir trees with the same diameter had different sapwood depths according to their location (coast area or interior land), and elevation [24].

Even though there is sufficient work supporting the strong relationships between a single tree's sapwood area and leaf area, these models cannot be used to scale up to large regions or stands. In a forested region, it is expected that leaf area increases as the ground area increases, and of course as the ground area increases, the greater likelihood of the area having multiple species. Therefore, it is insufficient to use a single tree model to interpolate either leaf area or sapwood area values for a group of trees composed of different species [25,26]. Thus, it is necessary to develop species specific models for the LA_{sp}:SA_{sp} relationship. More recent studies attempted to model *Eucaliptus regnans*' stand sapwood area-basal area ratios by scaling up individual stumps' visual heartwood-sapwood differentiation and using digital photography. They obtained a linear model with a coefficient of determination of 0.85 [27]). Modeled sapwood area at the stand level using LIDAR images and individual tree detection algorithms were used to predict sapwood area/basal area relationships at the stand level [28]. Their predicted values drew correlation coefficients that varied from 0.5 to 0.84, where the most adequate fit was with a regression model that combined LIDAR derived data and observed basal area. A mathematical model of a catchment's basal area-sapwood area was created by indirect estimates through LIDAR imaging [29].

Not all methods for estimating sapwood area will give the same results [30,31] and the direct or indirect measurement of leaf area may also produce different outcomes [32]. Given this, the research hypothesis in this study is that in addition to site conditions—such as stand density, climatic factors, and physical characteristics, the methods used to measure and estimate sapwood area and leaf area, significantly influence the LA_{sp}:SA_{sp} relationship and therefore, the calculation of the error propagated to the final estimate will determine the quality of an allometric model and help detect if the model contributes to over- or under-estimates. A thorough statistical analysis to determine the normality of each dataset, will help to determine if a regression model fits the dataset or whether other statistical/mathematical models should be considered. Hence, the objectives of this paper are: (1) To create reliable regression models—if adequate for each dataset—to estimate sapwood area at the breast height for *Populus tremuloides*, *Pinus banksiana*, *Pinus contorta*, *Picea glauca*, and *Picea mariana;* (2) to develop appropriate scaling *LA-SA* relationships for forest stands comprised of a mixture of these

species; and (3) to determine the absolute error propagated while scaling sapwood depth from an individual tree up to the stand level.

2. Materials and Methods

2.1. Model Approach and Sampling Design

For scaling purposes (from tree-to-stand level), a vegetated stand with vascular species has been conceptualized as an area of forested land (a stand) with a single tree with a sapwood area SA_{plot} equal to the summation of all the individual trees' sapwood cross-sectional area (SA_i) inside the stand.

$$SA_{plot} = \sum_{i=1}^{n} SA_i \quad (1)$$

where SA_i is species specific for each tree i in the stand containing n trees of different species. Similarly, the single tree's leaf area (LA_{plot}) will be the summation of all trees' leaf area inside the stand.

$$LA_{plot} = \sum_{i=1}^{n} LA_i \quad (2)$$

Despite the simplicity of the concept, it considers vegetation heterogeneity by using species specific models to scale up biophysical characteristics. At the tree-level, linear regression models were developed for each species sapwood depth $\overline{sd}$ versus outer bark diameter at breast height (D_{OB}) data so that Equation (3) below could be used to estimate SA_i:

$$SA_i = \pi\left(D_{OB_i}\overline{sd}_i - \overline{sd}_i^2\right) \quad (3)$$

where $\overline{sd}_i$ is each i^{th} tree's average sapwood depth and D_{OB_i} is the i^{th} tree's diameter at breast height. Equation (3) calculates SA_i as the region lying between two concentric circles within a tree's cross-section. The outermost circle borders the bark and vascular cambium, while the innermost one bounds the heartwood. These circles are naturally irregular but tree trunks are treated as having a cylindrical shape. The models obtained were used to estimate every tree's sapwood area SA_i inside the delimited stand. Equation (1) is then used to estimate the stand level sapwood area (SA_{plot}) of that single tree representing the whole stand. The correlation between species specific leaf area and sapwood area (LA_{sp}:SA_{sp}) and a mathematical scaling approach detailed in Section 3 were used to estimate LA_{plot}:SA_{plot}.

The leaf area for the stand LA_{plot}, was obtained by measuring the Leaf Area Index (LAI) by light transmission, and the surface ground area of interest. Stands of four different sizes are used to validate the LA_{sp}:SA_{sp} relationship. Four stands were 60 × 60 m, and nine were 10 × 10 m. These stands were located in the Sibbald Areas of Kananaskis Country, Alberta, Canada. The species composition of these stands was either dominated by deciduous trees (mainly *Populus tremulolides*), or coniferous trees (*Pinus contorta* and *Picea glauca*). Figures 1 and 2 show the location and delimitation of these stands. Two more stands were delimited at Whitecourt, in northern Alberta: One was dominated by *Pinus banksiana* individuals (20 × 20 m) and one was dominated by *Picea mariana* (15 × 15 m) individuals. The stands whose species composition was dominated by a conifer tree were labelled as "coniferous", and for those whose species composition was dominated by a deciduous tree were labeled as "deciduous". The 10 × 10 m stands were distinguished from the larger ones (≥ 300 m^2) by adding a prime symbol in front of their assigned number. Field data collected at each stand included: (a) Number of trees per stand, (b) species identification, and outer bark diameter at breast height for every tree inside the stand, and (c) Leaf Area Index for the stand. LAI was measured in the 60 × 60 m stands using the Tracing Radiation and Architecture Canopies (TRAC, 3rd Wave Engineering Co.;

Nepean, Ontario, Canada) device. The Canopy Analyzer LAI-2000 (LI-COR Incorporated; Lincoln, Nebraska, US) was used to measure LAI in the stands of 20 × 20 m and 15 × 15 m, located in Whitecourt.

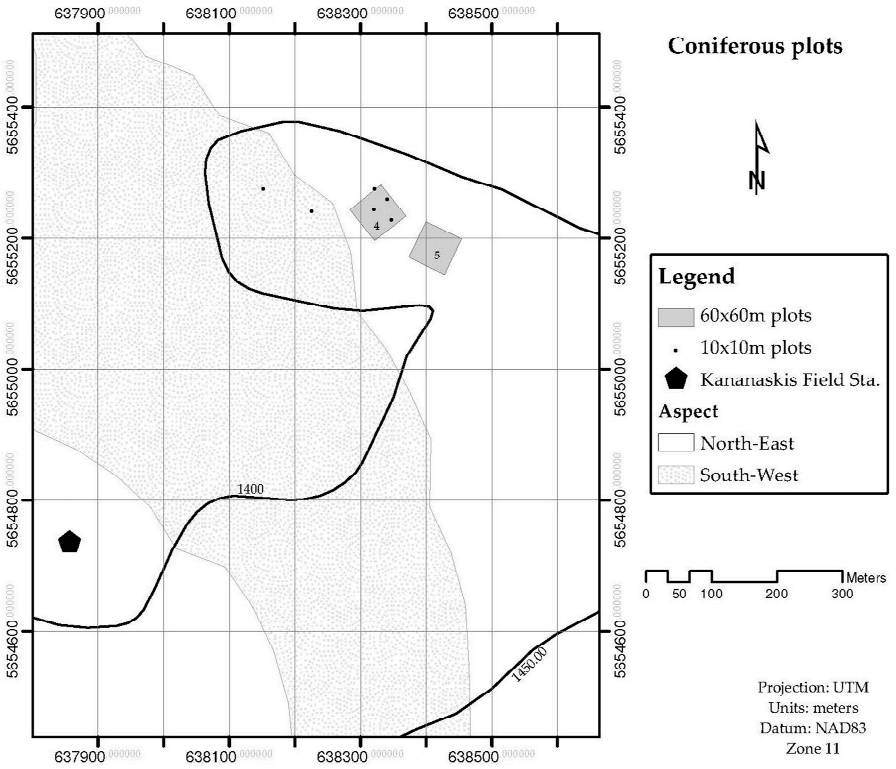

Figure 1. Geographical location of coniferous plots. The plots are in the Sibbald area, Kananaskis Country.

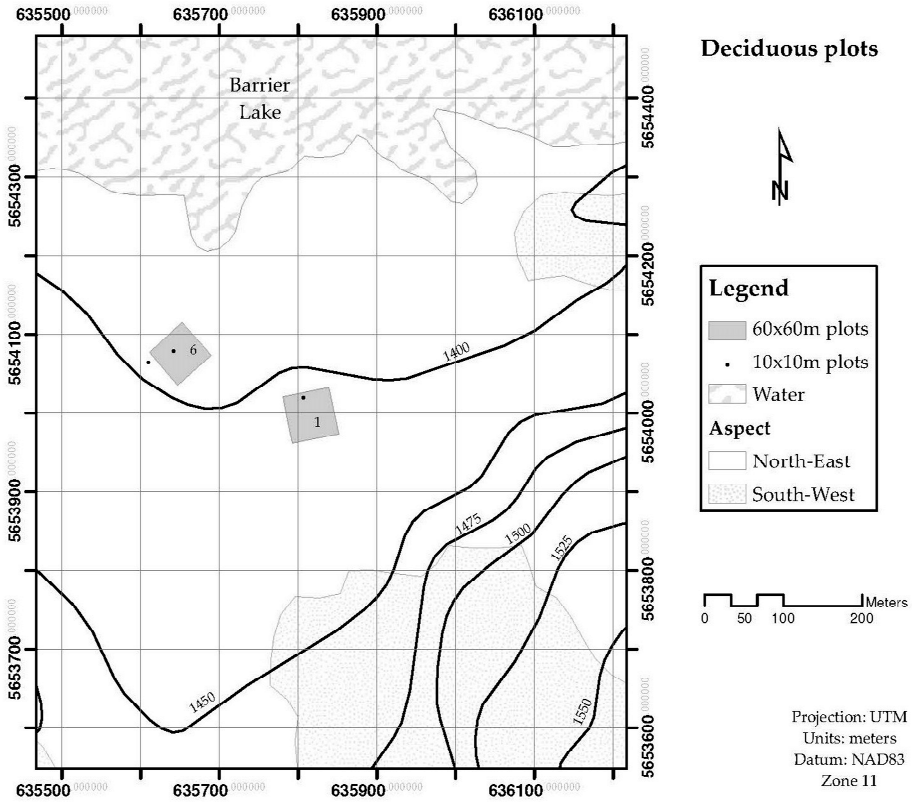

Figure 2. Geographical location of deciduous plots. The plots are in the Sibbald areas, south-east of Barrier Lake (Kananaskis Country).

Kananaskis Valley is a Montane closed forest formation [33] within the Rocky Mountains [34,35]. The Montane forest is classified as an ecoregion within the Cordilleran eco-province with a particular mix of physiography and air masses leading to unique climatic conditions [35]. Within Alberta, the Montane forest maintains the warmest temperatures during the winter than any other forested ecosystem. This type of forest has ridged foothills and a marked rolling topography. The Whitecourt forest is within the mid boreal mixed-wood ecoregion [35] and considered a closed forest formation [36] in the Southern Alberta uplands [35]. Further details on the field sites can be found in [31,37].

2.2. Treatment of Saplings

Since saplings generally lack heartwood and being mostly composed of sapwood [20,30,38], saplings correlations between D_{OB} and $\overline{sd}$, or between D_{OB} and cross-sectional area per species (SA_{sp}) will be different than for mature trees and thus, were treated separately. Furthermore, due to their size and composition, saplings were considered part of the understory, and this study focused on scaling allometric correlations of the overstory. Saplings were considered those trees with D_{OB} ranging between 2.41 cm and 10.2 cm, and heights between 38.1 cm and 76.2 cm. Trees found inside of the stands with a $D_{OB} \leq 10$cm were considered saplings, and were excluded from all allometric correlations.

2.3. Statistical Analysis

For each species, we performed statistical analyses to determine the most adequate regression model. These statistics include the Pearson's correlation coefficient, detection of outliers, the regression analysis, ANOVA, list of unusual observations, and the lack-of-fit test. Finally, each linear model's residuals were examined to check the model adequacy. Model adequacy checking included a normal plot of residuals and a plot of residuals versus fitted values.

In addition to the correlation analysis, a pairwise comparison of the coefficient of variation (COV) confidence intervals (C.I.) was used as an indication of the relationship between the scaling parameters at the stand scale (i.e., between SA_{plot} and LAI, and between SA_{plot} and LA_{plot}). The pairwise comparison consisted of comparing the parameters' C.I.s to see if they overlapped or not. This was another way to test if there was correlation between the variables. Because they are different parameters and the units differ, it was not suitable to use mean values or standard deviations to test the similarity between the two sample populations [39–41].

For 100 $(1 - \alpha)$% and $\nu = n - 1$ degrees of freedom, the modified McKay confidence interval for a COV [40] is:

$$\left[\left(\frac{u_1 + 2}{n} - 1\right)K^2 + \frac{u_1}{\nu}\right]^{-0.5} K \leq COV \leq K\left[\left(\frac{u_2 + 2}{n} - 1\right)K^2 + \frac{u_2}{\nu}\right]^{-0.5} \quad (4)$$

where K is the point estimate of COV ($K = \frac{S}{\overline{X}}$), $u_1 = \chi^2_{\nu,1-\alpha/2}$ and $u_2 = \chi^2_{\nu,\alpha/2}$. Therefore, K is a function of the sample standard deviation (S), and the sample mean ($\overline{X}$).

Another modified approach to MacKay C.I. is the suggested by [42]:

$$\chi^2_{\nu,1-\alpha/2}\left[\frac{1 + K^2}{nK^2}\right]^{-0.5} \leq COV \leq \chi^2_{\nu,\alpha/2}\left[\frac{1 + K^2}{nK^2}\right]^{-0.5} \quad (5)$$

3. Model Implementation and Data Results

For all five species, the tree-level sapwood depth was measured by microscopical analysis of wood anatomy to differentiate between sapwood and heartwood, as well as to differentiate sapwood from cambium and phloem. The sampling, sapwood depth, average sapwood depth, and D_{OB} results obtained for each species sampled to create the tree-level allometric correlations reported in [31].

3.1. Tree-Level Allometric Correlations

Pinus banksiana and *Pinus contorta* average sapwood depth $\overline{sd}$ was not well correlated with their respective D_{OB} [31]. This was also true of *Picea mariana*. *Picea glauca* and *Populous tremuloides* did however, show significant, positive linear correlations between $\overline{sd}$ and D_{OB}. For *Picea glauca*, the relationship from [31] and used here was:

$$\overline{sd} = 0.09D_{OB} - 0.70 \; R^2 = 0.84 \tag{6}$$

For *Populous tremuloides* the relationship obtained in [31] was used and is as follows:

$$\overline{sd} = 0.24D_{OB} + 0.92 \; R^2 = 0.52 \tag{7}$$

Depending on the correlation between $\overline{sd}$ and D_{OB} (that is, whether there is no relationship or a significant linear relationship like those shown in Equations (6) and (7)), the methods for scaling up to the stand level using D_{OB} required a species-based approach. Thus, for *Picea glauca* and *Populous tremuloides*, Equations (6) and (7) were used to determine stand level $\overline{sd}$ estimates from stand level estimates of D_{OB}, respectively. For those species without a strong tree-level linear correlation, a simple stand average, i.e., $\overline{sd}$, was proposed.

3.2. Stand-Level Allometric Correlations

3.2.1. Scaling Up Sapwood Area from the Tree to the Stand Level

Since it was feasible to fit a linear regression model for two of the five studied species, the aggregation of cross-sectional sapwood area to the stand level to obtain SA_{plot} was performed by fusing two approaches. To estimate the sapwood area at every stand, if *Picea glauca* and/or *Populus tremuloides* trees were present, their respective linear model was applied—this was the first scaling approach. But under the presence of *Pinus banksiana* and/or *Pinus contorta* and/or *Picea mariana*, their respective average sapwood area was applied, which is the second scaling approach. Therefore,

$$SA_{plot} = \sum_{j=1}^{L} SA_j + \sum_{k=1}^{M} SA_k \tag{8a}$$

which is further expanded as (8b):

$$SA_{plot} = \sum_{j=1}^{L} \sum_{i=1}^{N_{sp,j}} \left[D_{OB_{i,j}} \overline{sd}'_{i,j} - \left(\overline{sd}'_{i,j} \right)^2 \right] \pi + \sum_{k=1}^{M} \overline{SA}_k N_{sp,k} \tag{8b}$$

where L is the number of species present with a linear model (i.e., L = 0, 1 or 2 depending on whether none, one, or both are present of *Picea glauca* or *Populus tremuloides*; thus, if L = 0, the summation with j beginning at 1 is null), $N_{sp,j}$ is the total number of trees inside the stand of species j; $D_{OB_{i,j}}$ is the i^{th} individual's D_{OB} of species j; and $\overline{sd}'_{i,j}$ is the i^{th} individual's estimated sapwood depth for species j, and estimated for trees of species *Picea glauca* with Equation (6), or *Populus tremuloides* with Equation (7). The second term on the right-hand side of Equation (8a) pertains to those species that did not produce a significantly linear model. Thus, M is the number of species k present in the stand with k being *Pinus banksiana*, *Pinus contorta*, or *Picea mariana*. M = 0, 1, 2 or 3; and $N_{sp,k}$ is the number of trees in the stand of each of these species. Based on previous results [31], it was assumed that the sapwood cross-sectional area for each of these three species remained relatively constant as the tree grew. Therefore, for each of these species k, the average sapwood area was calculated based on results from [31] with important details given in the next paragraph for $\overline{SA}_k$.

The study of [31] determined what relationships existed for these five boreal species between $\overline{sd}$ and D_{OB}. Microscopically differentiated average sapwood depth (averaged over the four cardinal directions) from wood cores obtained for the fives species was correlated with D_{OB} for each tree in that study. Average sapwood area for each species that did not have a linear relationship between $\overline{sd}$ and D_{OB} was computed using Equation (9):

$$\overline{SA}_k = \frac{\sum_{i=1}^{t_k}\left[D_{OB_{i,k}}\overline{sd}_{i,k} - \left(\overline{sd}_{i,k}\right)^2\right]\pi}{t_k} \quad (9)$$

where, $\overline{sd}_{i,k}$ is the average sapwood depth for each cored tree i, of species k, in that study, and accordingly, $D_{OB_{i,j}}$ was the outer bark diameter at breast height for tree i of species k and t_k was the number of cored trees in the sample sets of [31]. Values of $\overline{SA}_k$ and t_k for all five species are reported in Table 1 and [31] provides greater details not contained here.

Table 1. Values of average tree-level sapwood area for each species computed with data from [31]. Only for the first three species on the list, $\overline{SA}_k$ was used to estimate stand level (SA) in Equation (8b).

Species (k)	t_k	$\overline{SA_k}$ (cm^2)
Pinus banksiana and *Pinus contorta*	33	176.47
Picea mariana	21	213.57
Populus tremuloides	26	277.13
Picea glauca	17	277.52

The SA_{plot} calculated for each 60 × 60 m and 10 × 10 m stand, including tree species, tree quantity, stand D_{OB} statistics and the error associated with SA_{plot}, are given in Tables 2 and 3, respectively. The conifer sites were those sites containing *Picea glauca*, *Pinus contorta*, *Pinus banksiana*, and *Picea mariana*. The deciduous sites were mainly composed of *Populus tremuloides*. If deciduous individuals were present in the coniferous stands, their numbers counted for less than 10% of the total tree quantity or were mainly saplings. Such was the case of the site Conifer-5, with a *Populus tremuloides* tree quantity of 114; however, 92 individuals were saplings. Thus, the count of deciduous trees inside the stand was a small portion of the total in terms of sapwood area contribution. Most of the deciduous sites were 100% pure stands, and if any other tree was present, it counted for less than 5% of the total stand's tree quantity (e.g., Deciduous-6). Most of the coniferous sites (60 × 60 m and 10 × 10 m) were composed of *Picea glauca* and *Pinus contorta* trees. The two pure coniferous sites were Conifer-11 and Conifer-12.

Table 2. Descriptive statistics of the 60 × 60 m stands located in the Sibbald areas of Kananaskis Country, Alberta, and Whitecourt, Alberta. Tree quantity is either $N_{sp,k}$ or $N_{sp,j}$ depending on the species; SA_{sp} is either SA_j or SA_k in Equation (8b), depending on the species, ΔSA_{plot} is the absolute error associated with SA_{plot}. D_{OB} units are in cm, and all areas are in units of m^2.

Plot	Tree species	No. of Trees	Max. D_{OB}	Min. D_{OB}	Avg. D_{OB}	SA_{sp}	SA_{plot}	ΔSA_{plot}
Conifer-4 [1]	*Picea glauca*	434	43.3	2.2	13.14	2.92		
	Pinus contorta	276	33.42	5.73	20.15	4.87	7.79	± 0.03
Conifer-5 [1]	*Picea glauca*	164	48.38	2.86	18.31	2.29		
	Pinus contorta	48	26.1	1.59	14.09	0.85		
	Populus tremuloides	114	19.42	2.86	7.23	0.14	3.28	± 0.03
Conifer-11 [2]	*Pinus banksiana*	129	25.15	6.37	16.57	2.28	2.28	± 0.03
Conifer-12 [2]	*Picea mariana*	60	23.55	5.09	15.69	1.28	1.28	± 0.01
Deciduous-1 [1]	*Populus tremuloides*	83	25.46	9.55	18.57	1.45	1.45	± 0.01
Deciduous-6 [1]	*Populus tremuloides*	498	31.19	8.91	19.1	9.37		
	Picea glauca	14	48.38	7	23.4	0.18	9.55	± 0.08

[1] Indicates Sibbald region of Kananaskis Country and [2] indicates Whitecourt region.

Table 3. Descriptive statistics of the 10 × 10 m stands (indicated with a prime symbol) located in the Sibbald areas of Kananaskis Country, Alberta. Note, ΔSA_{plot} is the absolute error associated with SA_{plot}. The error propagation estimation is detailed in Section 3.3. D_{OB} units are in cm, and all areas are in units of m^2.

Plot	Tree Species	No. of Trees	Max. D_{OB}	Min. D_{OB}	Avg. D_{OB}	SA_{sp}	SA_{plot}	ΔSA_{plot}
Conifer-1′	*Picea glauca*	29	24.51	5.091	6.53	0.16		
	Pinus contorta	12	26.74	14.01	19.89	0.21	0.37	± 0.001
Conifer-2′	*Pice glauca*	15	27.06	7.641	14.88	0.21		
	Pinus contorta	9	27.37	16.23	20.23	0.16	0.37	± 0.001
Conifer-3′	*Picea glauca*	19	25.78	4.461	12.48	0.19		
	Pinus contorta	13	29.6	10.82	19.98	0.23	0.42	± 0.0007
Conifer-4′	*Picea glauca*	9	21.33	3.501	12.59	0.04		
	Pinus contorta	14	27.06	11.78	20.35	0.25	0.29	± 0.0003
Conifer-5′	*Picea glauca*	4	28.33	12.41	18.94	0.05		
	Pinus contorta	13	32.79	15.92	22.33	0.23	0.28	± 0.0002
Conifer-10′	*Picea glauca*	5	33.74	5.091	16.87	0.19		
	Pinus contorta	14	34.7	12.73	21.99	0.11		
	Populus tremuloides	1	21.01			0.02	0.32	± 0.0005
Deciduous-7′	*Populus tremuloides*	31	32.79	9.871	17.15	0.34	0.34	± 0.004
Deciduous-8′	*Populus tremuloides*	28	28.01	14.01	20.29	0.59	0.59	± 0.005
Deciduous-9′	*Populus tremuloides*	22	23.24	14.64	19.92	0.43	0.43	± 0.004

3.2.2. Leaf Area Estimates at the Stand-Level

Leaf Area Index, LAI, was measured in the 60 × 60 m stands with the Tracing Radiation and Architecture Canopies (TRAC, 3rd Wave Engineering Co.; Nepean, Ontario, Canada) device. At the two stands located in Whitecourt (Conifer-11, Conifer-12), the Effective Leaf Area Index, LAI_{eff}, was measured with the Canopy Analyzer LAI-2000 (LI-COR Incorporated; Lincoln Nebraska, US. To convert LAI_{eff} to Leaf Area Index (LAI), we applied Chen's equation [43]:

$$\mathrm{LAI} = (1 - \alpha_l)\mathrm{LAI}_{\mathrm{eff}}\gamma_E\Omega_E \tag{10}$$

where α_l is the woody-to-total area ratio (i.e., tree's woody fraction), γ_E is the needle-to-shoot area ratio (i.e., fraction of needles per shoot), Ω_E is the clumping index. In order to derive the α_l and γ_E values from the typical values reported by [44], the age and productivity of the stand must be known. Thus, age and productivity characteristics were defined by comparing the LAI_{eff} with typical values reported in [45]. The LAI_{eff} of the *Pinus banksiana* stand was similar to an intermediate/medium productivity stand (LAI_{eff} = 2.20) with α_l of 0.05 and γ_E of 1.35. The *Picea mariana* stand LAI_{eff} value was similar to a mature medium/high productivity stand (LAI_{eff} = 2.78), thus, α_l is assumed as 0.14 and γ_E as 1.35. Finally, Ω_E was derived from typical values reported by [45] as well; thus, the Ω_E values for *Picea mariana* and *Pinus banksiana* were respectively set as 0.65 and 0.75. The fifteen stands estimated LAI (LAI_{plot}) concur with the previous reported values by [43,45,46].

The total leaf area per stand, LA_{plot} was estimated based on the definition of Leaf Area Index: "The total one-sided (or one half of the total all-sided) green leaf area per unit ground surface area":

$$LA_{plot} = (\mathrm{LAI})A_{plot} \tag{11}$$

Table 4 displays the estimates of LAI_{plot}. The coniferous 10 × 10 m stands' areas were adjusted and reported as 150 m^2 in order to take into account what is known as the "TRAC footprint". The TRAC footprint was created by trees with shadows large enough to fall into the delimited stand influencing the TRAC measurements. Thus, the LAI measured in the field belonged to a larger area than the delimited one. This effect was not evident in the 10 × 10 m deciduous stands. Furthermore, the TRAC footprint was influenced by tree height and solar zenith angle (θ) [44]. Therefore, the TRAC footprint was adjusted by assuming that in Kananaskis Country, the coniferous trees' average height was approximately 15 m, and the solar noon zenith angle was about 45.21° on the date when LAI was

measured (day 238 of the year). Therefore, the extent of the footprint (tree height × tanθ) was 15 m. This extent would occur in only one side of the stand giving an LAI for a stand area of 10 × 15 m.

Table 4. Leaf Area Index (LAI) and estimated LA_{plot} according to stand size where ΔLA_{plot} is the absolute error associated with LA_{plot}. The error propagation estimation is detailed in Section 3.3. Prime symbol indicates 10 × 10 m stands. No prime symbol indicates 60 × 60 m stands.

Site	*LAI*	Plot Size (m^2)	LA_{plot} (m^2)	ΔLA_{plot} (m^2)
Conifer-1′	6.90	150	1035.00	± 19.90
Conifer-2′	6.04	150	906	± 19.04
Conifer-3′	6.57	150	985	± 19.57
Conifer-4′	5.34	150	801	± 18.34
Conifer-5′	4.51	150	676.5	± 17.51
Conifer-10′	6.12	150	918	± 19.12
Conifer-4	5.71	3600.00	20,556.00	± 1338.20
Conifer-5	2.54	3600.00	9144.00	± 855.10
Conifer-11	3.76	400	1502.52	± 259.32
Conifer-12	4.96	300	1486.97	± 242.82
Deciduous-1	2.64	415	1093.53	± 405.85
Deciduous-6	3.14	3600,00	11,304.00	± 1144.27
Deciduous-7′	2.30	100	230	± 12.30
Deciduous-8′	3.57	100	357	± 13.57
Deciduous-9′	3.22	100	322	± 13.22

3.2.3. Stand Level Leaf Area Sapwood Area Allometric Correlations

In the case of the *Populus tremuloides* sites, a close similarity was found between the two sets of stands of 10 × 10 m and 60 × 60 m in terms of LAI. In order to support this observation, the equality of variances with Bartlett's test and the F-test was conducted. Based on the two statistical test results, the LAI variances of the two sample sets were equal (C.I. = 95%) and the two sets were merged to observe the correlation of *Populus tremuloides* leaf area and sapwood area at the stand level. The explanation for such a similarity between *Populus tremuloides*' leaf area at different scales may be related to the canopy type. Unlike coniferous trees, *Populus tremuloides* canopy is horizontally wide, creating small gaps between the canopy of neighboring trees. This effect of *Populus tremuloides* canopies is due to their wide-circular leaves and their alternate (not clumped) distribution. At the same time, the leaves are predominantly at the top of the tree, creating a rounded crown with a large diameter. Moreover, in the studied sites, the *Populus tremuloides* tree heights were all similar. The combination of these characteristics gives wider tree shadows that practically cover the entire stand's floor at noon. Thus, inside the stand there is little room for observing the footprint of external trees in any direction meaning that the TRAC device mostly measures the LAI inside the stand with a negligible footprint. This was proven by examining the LAI measured in the east–west and north–south transects. In both east–west and north–south directions, LAI was observed to have practically the same value (a paired T-test proved that the difference of the population mean was equal to zero with an $\alpha = 0.05$). Hence, it was concluded that it was possible to merge both data sets for use in a linear regression model.

For all *Populus tremuloides* sites, there was a strong linear correlation between SA_{plot} and LA_{plot} ($\rho \approx 0.999$), and the p-value that equaled zero gave sufficient evidence to conclude that the correlation was not zero ($\alpha = 0.05$). Results of the regression analysis supported the decision of fitting a linear model to the data, showing that LA_{plot} resulted in a significant predictor of SA_{plot} with a p-value < 0.0001 ($\alpha = 0.05$). The ANOVA results determined that LA_{plot} contributes significantly to the model ($\alpha = 0.05$). The first fitted model (Figure 3) had a high coefficient of determination ($R^2 = 99.8\%$) that supported the theory of SA_{plot} being fairly well explained by a linear model. The R^2_{adj} (99.8%) was close in value to the R^2. The R^2_{pred} (57.77%) was weak with a large difference from R^2_{adj}. Thus, there was a slight indication of one value inflating the prediction, and thus, this model might not be suitable for other stands. The list of unusual observations draws attention to the large influence

that the Deciduous-6 site gives to the model, considering it was an unusual observation. Even if the observation was not considered an outlier, it was removed from the sample set, and the regression model was fitted with only the four observations. In the second regression attempt (Figure 4), all the coefficients of determination values were lower than the ones of the first model. The R^2 was high (99.2%), and the R^2_{pred} (79.5%) was in reasonable agreement with the R^2_{adj} (98.78%). Thus, the second model was proposed for practical use.

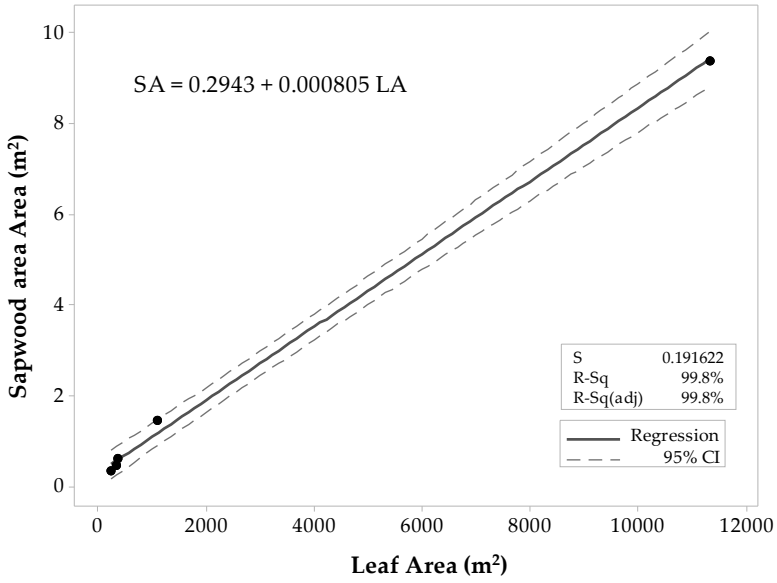

Figure 3. Fitted linear regression model for *Populus tremuloides* predicted SA_{plot} in relation to its LA_{plot}. This model includes all 60 × 60 m and 10 × 10 m stands.

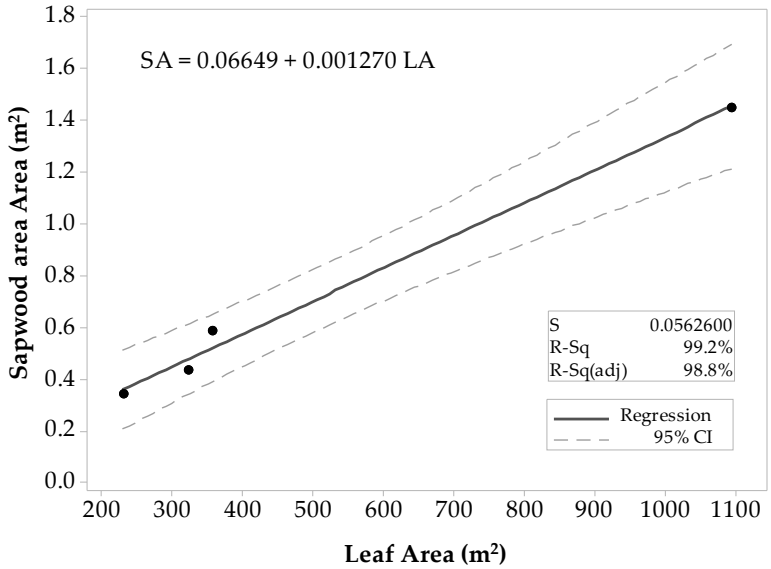

Figure 4. Fitted linear regression model for *Populus tremuloides* predicted SA_{plot} in relation to its LA_{plot}. This model does not include the stand Deciduous-6.

The coniferous SA_{plot} and LA_{plot} estimates for the 10 × 10 m and 60 × 60 m stands are given in Table 5. For all coniferous sites, there was a strong linear correlation between the SA_{plot} and the LA_{plot}, and the *p*-value supports that the correlation is not zero. However, if a regression model was derived by using both sample sets (10 × 10 m and 60 × 60 m stands), the lack-of-fit test is significant at a *p*-value of 0.019. The lack-of-fit test suggested a possible curvature in the model and that some other type of model should be fitted. It was assumed that the mismatch between the two data sets was due

to the overestimation of LAI due to the influence of the footprint at the 10 × 10 m scale. Therefore, the sapwood area for the 10 × 10 m stands were underestimated between 20% and 29.6%. Hence, in the case of the coniferous sites, the obtained values for the 10 × 10 m stands were not suitable for combination with the 60 × 60 m stands because of the footprint caused by the canopy type (which was not randomly distributed, that is, it was clumped, and had large open areas that allow trees outside of the stand to reflect their shadows inside of it).

Table 5. Estimated sapwood area and their respective leaf area per stand, conifer sites. The first six sites are of size 10 × 10 m while the last four are of 60 × 60 m.

Site	SA_{plot} (m^2)	LA_{plot} (m^2)	Pearson's Correlation Coefficient, (*p*-Value)
Conifer-1′	0.37	1035	
Conifer-2′	0.37	906	
Conifer-3′	0.42	985.5	
Conifer-4′	0.29	801	
Conifer-5′	0.28	676.5	
Conifer-10′	0.33	918	
			0.85 [1], (0.033)
Conifer-4	7.79	20,556.00	
Conifer-5	3.28	9144.00	
Conifer-11	2.28	1502.52	
Conifer-12	1.28	1486.97	
			0.98 [2], (0.022)
			0.97 [3], (<0.001)

[1] Correlation between 10 × 10 m stands, [2] correlation between 60 × 60 m stands, [3] correlation includes all stands.

The sample set was then divided into the 10 × 10 m and the 60 × 60 m stands to fit two separate regression models for the conifer stands. The first model corresponded to the 10 × 10 m stands (Figure 5), and the latter model was fit for the 60 × 60 m stands (Figure 6). Regression analysis and ANOVA results suggest that the LA_{plot} is a significant predictor of the SA_{plot} (α = 0.05). However, the model's R^2_{pred} for the 10 × 10 m stands denote inadequacy for future predictions, and the R^2_{pred} (38.37%) significantly differs from the R^2_{adj}. The regression model for the 60 × 60 m stands, however, show a better agreement between its coefficients of determination (Figure 6). Still the difference between R^2_{adj} and the R^2_{pred} was large (68.60%), but the model adequacy check gave enough evidence to support the decision for fitting a linear model to the 60 × 60 m data set. Both models have similar slopes that differ by just about 0.37 cm^2.

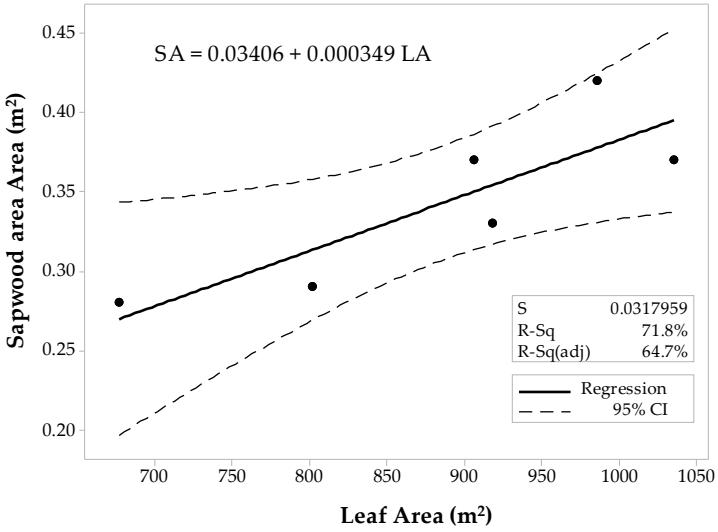

Figure 5. Fitted linear regression model for the 10 × 10 m stands of conifers, SA_{plot} in relation to its LA_{plot}.

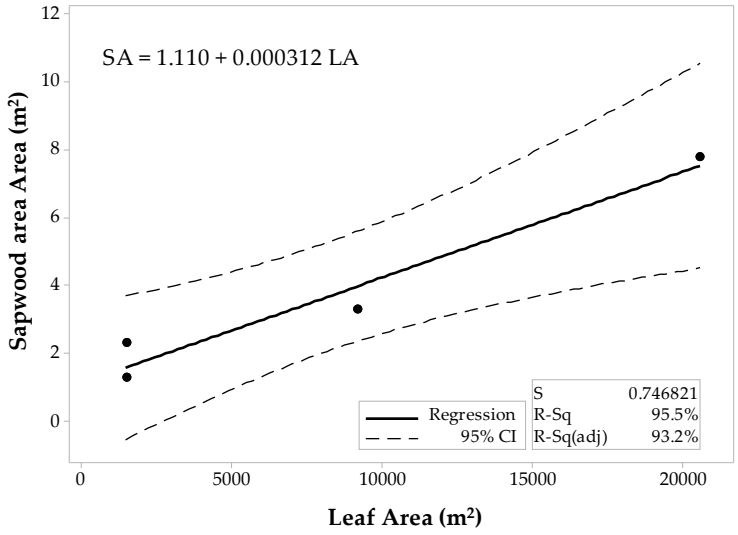

Figure 6. Fitted linear regression model for the 60 × 60 m stands of conifers, SA_{plot} in relation to its LA_{plot}.

3.2.4. COV Confidence Intervals

The pairwise comparison of C.I. for COV was an extra analysis to support the applicability and reliability of the regression models, because the sample size for both data sets was not as large as desired when fitting a linear regression model. Therefore, this analysis reinforced the suggested relationship between the scaling factors, no matter the sample size. Since most of the COVs were larger than 0.33, Payton's equation (Equation (4)) was used to estimate the C.I. Table 6 displays the obtained COVs and C.I. of SA_{plot}, LAI, and LA_{plot}.

Table 6. Coefficient of variation (COV) results for the coniferous and deciduous stands' SA_{plot}, LA_{plot} and LAI with their 95% confidence intervals (95% C.I.s).

Site Type	Variable	COV	95% C.L.
Coniferous	SA_{plot}	0.72	0.4963–1.6222
	LA_{plot}	0.79	0.5943–1.9426
	LAI	0.32	0.2438–0.7976
Deciduous	SA_{plot}	1.46	0.6614–1.7885
	LA_{plot}	1.82	0.7026–1.8999
	LAI	0.17	0.1344–0.3633

For the coniferous data set, the LA_{plot}, SA_{plot}, and LAI confidence intervals were not significantly different; therefore, this suggested that there may be correlations amongst these scaling factors. For the deciduous data set, the LA_{plot} and SA_{plot} confidence intervals were not significantly different, while the LAI confidence interval was significantly different from the LA_{plot} and SA_{plot} confidence intervals. Therefore, this may be an indication of a correlation between LA_{plot} and SA_{plot} but there should be no correlation between SA_{plot} and LAI in the deciduous data set. These results were in reasonable agreement with the results obtained with the Pearson's correlation hypothesis test and the regression analysis.

3.3. Estimates of Error Propagation

The absolute error on SA_{plot} estimates (ΔSA_{plot}) was calculated based on the rules of error propagation that are derived from a Taylor series [47]. Equation (8a) describes SA_{plot} as the summation of each tree's SA, thus, ΔSA_{plot} will be given by the summation of each tree's error contribution to SA:

$$\Delta SA_{plot} = \sum_{i=1}^{T}\left[\left|\frac{\partial SA_{plot}}{\partial D_{OB_i}}\right|\Delta D_{OB_i} + \left|\frac{\partial SA_{plot}}{\partial \overline{sd}'_i}\right|\Delta\overline{sd}'_i\right] \tag{12}$$

where ΔD_{OB_i} and $\Delta\overline{sd}'_i$ are the absolute errors on the i^{th} tree's D_{OB} and estimated $\overline{sd}_i$, respectively. The measurement of D_{OB} were carefully verified by measuring the circumference of the trees at breast height on the same tree, 50 times. Two trees were measured in this exercise. The average error calculated was ± 0.0024 m.

For *Picea glauca* $\overline{sd}$ estimates (Equation (6)), $\Delta\overline{sd}'_i$ will be given by:

$$\Delta\overline{sd}'_i = \left|\frac{\partial\overline{sd}'_i}{\partial D_{OB_i}}\right|\Delta D_{OB_i} = 0.09\Delta D_{OB_i} \tag{13}$$

In the *Populus tremuloides* linear model (Equation (7)), $\Delta\overline{sd}'_i$ is given by:

$$\Delta\overline{sd}'_i = \left|\frac{\partial\overline{sd}'_i}{\partial D_{OB_i}}\right|\Delta D_{OB_i} = 0.24\Delta D_{OB_i} \tag{14}$$

Solving the partial derivatives in Equation (12) and substituting $\Delta\overline{sd}'_i$ for Equation (13), the *Picea glauca* ΔSA_{plot} is:

$$\Delta SA_{plot} = \sum_{i=1}^{T}\left[\left(\overline{sd}'_i\Delta D_{OB_i}\right) + \left(\Delta D_{OB_i} - 2\overline{sd}'_i\right)0.09\Delta D_{OB_i}\right] \tag{15}$$

and for *Populus tremuloides*:

$$\Delta SA_{plot} = \sum_{i=1}^{T}\left[\left(\overline{sd}'_i\Delta D_{OB_i}\right) + \left(\Delta D_{OB_i} - 2\overline{sd}'_i\right)0.24\Delta D_{OB_i}\right] \tag{16}$$

For the other three species studied here that have no linear relationship between average sapwood depth and diameter at breast height, ΔSA_{plot} was estimated by the following equation:

$$\Delta SA_{plot} = \left|\frac{\partial SA_{plot}}{\partial\overline{SA}_{sp}}\right|\Delta\overline{SA}_{sp} + \left|\frac{\partial SA_{plot}}{\partial T}\right|\Delta\mathrm{T} \tag{17}$$

Due to the direct method used in this study to measure T—the total number of trees inside a particular plot, it was considered an exact number (if some other approaches are used to indirectly estimate tree quantity, there may be an error associated with T); therefore,

$$\Delta SA_{plot} = T\Delta\overline{SA}_{sp} \tag{18}$$

where $\Delta\overline{SA}_{sp}$ is the absolute error on the SA average value and is given by:

$$\Delta\overline{SA}_{sp} = \sum_{i=1}^{n}\left[\left|\frac{\partial\overline{SA}_{sp}}{\partial D_{OB_i}}\right|\Delta D_{OB_i} + \left|\frac{\partial\overline{SA}_{sp}}{\partial\overline{sd}}\right|\Delta\overline{sd} + \left|\frac{\partial\overline{SA}_{sp}}{\partial n}\right|\Delta n\right] \tag{19}$$

where n is a constant; thus, the third term is null. The equation then becomes:

$$\Delta\overline{SA}_{sp} = \sum_{i=1}^{n}\left[\frac{\left(\overline{sd}_i\Delta D_{OB_i}\right) + \left(D_{OB_i} - 2\overline{sd}\right)\Delta\overline{sd}_i}{n}\right] \quad (20)$$

According to previous research, the measure of sapwood depth with the microscopical analysis of wood anatomy gives an accuracy of 98% [48]. The sapwood depth measurements supporting this research were obtained from [37] and were measured using the microscopical method. It was estimated that the error on $\overline{sd}$ was related to the accuracy of the ocular scale of the microscope (with divisions of 1μ) and the ruler (with divisions of 1 mm) used to measure each core's sapwood depth [37]. Thus, the instrument limit of error (ILE) was estimated as half of the smallest measuring increment of the instrument (ruler). Hence, it was estimated that $\Delta\overline{sd}_i$ = ILE = $\frac{1}{2}$(1 mm) = ± 0.0005 m. $\Delta\overline{SA}_{sp}$ for the *Pinus contorta* and *Pinus banksiana* sample set was 0.0002 m^2; $\Delta\overline{SA}_{sp}$ for the *Picea mariana* sample set was also 0.0002 m^2. Tables 2 and 3 report ΔSA_{plot} for the coniferous and deciduous sites, respectively.

Equation (21) is used to estimate the error on LA_{plot} (ΔLA_{plot}):

$$\Delta LA_{plot} = \left|\frac{\partial LA_{plot}}{\partial LAI}\right|\Delta LAI + \left|\frac{\partial LA_{plot}}{\partial A_{plot}}\right|\Delta A_{plot} \quad (21)$$

ΔLAI was ±0.10 for the deciduous stands and ±0.13 for the coniferous stands, while ΔA_{plot} was given by:

$$\Delta A_{plot} = \left|\frac{\partial A_{plot}}{\partial L}\right|\Delta L \quad (22)$$

Thus, on the whole we obtain:

$$\Delta A_{plot} = 2L\Delta L \quad (23)$$

where L is the stand's length, with ΔL = ±2.79 m for deciduous stands and ΔL = ±1.27 m for coniferous stands. The 10 × 10 m stands ΔL = ±0.05 m. Solving Equation (23), a deciduous 60 × 60 m stand's ΔA_{plot} was ±334.80 m^2 and ±138.26 m^2 for the 415 m^2 stand. A coniferous stand of 60 × 60 m had a ΔA_{plot} of ±152.40 m^2. Notice that ΔA_{plot} of the stands named Conifer-11 and Conifer-12 (from Whitecourt) were ±50.8 m^2 and ±44.45 m^2, respectively (because they had a smaller surface area). For the 10 × 10 m deciduous stands, ΔA_{plot} equaled ±1.00 m. The errors on LA_{plot} estimates are given in Table 4. Notice that the ΔLA_{plot} became larger as the stand size increased, being more notorious in the larger stands. In addition, the contribution of ΔLAI to ΔA_{plot} was small, but still the size of the stand influenced the first term of the Equation (21); however, if LAI increased in large stands, then ΔA_{plot} became large (e.g., Conifer-4, Deciduous-6).

The prediction of SA_{plot} for deciduous and coniferous stands using the obtained linear models, establishes that SA_{plot} = f(LA_{plot}). Thus, the error propagation on the linear models follows:

$$\Delta SA'_{plot} = \left|\frac{\partial SA_{plot}}{\partial LA_{plot}}\right|\Delta LA_{plot} \quad (24)$$

For the deciduous sites linear model, the ΔSA_{plot} produced the following:

$$\Delta SA'_{plot} = 0.00127\Delta LA_{plot} \quad (25)$$

For the coniferous linear model, the error on the SA_{plot} was:

$$\Delta SA'_{plot} = 0.000312\Delta LA_{plot} \quad (26)$$

4. Discussion and Conclusions

Reliable estimates of tree and stand sapwood area are necessary in the calculation of other eco-hydrological parameters such as the actual transpiration from trees, for example. The error associated with the estimates of SA and SA_{plot} will influence transpiration values if used to scale tree sap flow measurements. Since the accuracy of water balance components is crucial in this area of work, the authors believe that determining SA, SA_{plot}, LA and LA_{plot} propagated errors are fundamental to any such research and modelling. A number of studies have already highlighted the relevance of creating reliable allometric models, and have analyzed the error associated with their allometric correlations in order to support their reliability [26,49–51].

Regarding the allometric correlations, previous research [31] demonstrated that it was feasible to estimate a single tree's sapwood area for *Picea glauca* and *Populus tremuloides* using estimates of $\overline{sd}$ from D_{OB}. In this study, D_{OB} was not an adequate sapwood area predictor of *Pinus banksiana*, *Pinus contorta* and *Picea mariana* species. As a result, scaling cross-sectional sapwood area to the stand-level was approached by combining the estimates of SA obtained with the regression models for *Picea glauca* and *Populus tremuloides*, and by using an average of the sapwood area of the remaining three species in a combined approach that scaled up sapwood area from a single tree to the stand scale. To the authors' knowledge, the use of average sapwood area has not been previously studied as an option for scaling key, characteristic dimensions of trees. This combined approach gives reliable SA_{plot} estimates that were significantly correlated to LA_{plot} estimates derived from measurements of LAI. The final relationship (for both groups conifers and deciduous) allowed the development of linear models for predicting SA_{plot} as function of LA_{plot}. We attribute the reliability of the average sapwood area values to the careful and detailed methods that were used to measure a single tree's sapwood depth, and that contributed to an error that was almost negligible [31]. This statement was supported by a more recent research study that reached similar conclusions regarding accurate measures of sapwood depth [52].

The errors associated with the SA_{plot} estimates were mainly influenced by the size of the stand that in turn influenced the LA_{plot} values—the larger the plot, the more the associated error with LA_{plot}. This error (ΔLA_{plot}) had an impact on the estimates of SA_{plot} having LA_{plot} as predictor, and prevented stronger regression models by combining the 10 × 10 m and the 60 × 60 m coniferous stands. On the contrary, in the case of the *Populus tremuloides*, the addition of stands of a size in between 10 × 10 m and 60 × 60 m would improve the model even further and may allow it to be applicable for use on other data sets; and perhaps even allow the addition of the stand Deciduous-6 to the model. Another important point is that the reduction of error on leaf area estimates depends on accurate delimitation of the stands, and as the stand's size increases, it is more complicated to retain accurate stand delimitation. Still, stands larger than 10 × 10 m are needed in order to limit discrepancies associated with the footprint on LAI. Even though small stands give the smallest errors, there are large discrepancies between estimates of LA_{plot} and SA_{plot} due to the footprint influence. Consequently, we consider the analysis of the regression model for the 10 × 10 m stands helps to support the reliability of the 60 × 60 m linear models (since both follow the same linear pattern and the slope is practically the same). For future modelling, it might be suitable to add the slope as another predictor of sapwood area to the stand level, as suggested by [53] who determined that it is the slope that determines the correlation between stand-level leaf area and sapwood area. The authors recommend that at least for conifer trees, it is preferred to use stands that are bigger than 100 m^2, and by trying to reduce the footprint influence on LAI derived from optical measurements. Furthermore, attention to the accuracy in the relationship between D_{OB} and sd cannot be understated. In a simple computation to determine SA in the plots when simply using an average sapwood area (Equation (9)) for all species as opposed to Equation (9) only for *Pinus contorta, Pinus banksiana* and *Picea mariana* and the appropriate linear form of Equation (8) for *Populus* and *Picea glauca*, significant overestimates of SA were found (results not shown here). This in turn created an overestimate of the slope in the *LA:SA* models (as in Figures 3–6) for each set of plots.

Recent studies have stressed the significant influence that scaled values of sapwood area can exert on final estimates of tree transpiration [54]. Thus, studies that have carefully analyzed the different methods to scale up tree morphological characteristics and their associated uncertainty, as in this paper, this should be a good reference for choosing reliable scaling methods in order to reduce the error that may be propagated into stand, ecosystem, or even watershed estimates. It is also recommended that the errors associated with estimates of tree transpiration for instance, should be determined and added into the overall error propagation equation. Some studies have, however, focused on taking into account the errors associated with only a section of their models [54,55]. For reliability purposes, the authors strongly recommend that one determine all the errors associated with every single parameter of a scaling model.

In conclusion, these results establish the uniqueness of each species sapwood area, D_{OB} and *LA* allometries. Thus, any attempt to use the reported correlations in this paper for other estimates should do so for similar site conditions, topographic and climatic characteristics. In this study, it was possible to aggregate cross-sectional sapwood area from the tree to the stand level in a mixed forest by differentiating between deciduous and coniferous groups of trees, and by combining two different approaches, with an error that is considered negligible.

In terms of scaling, the results suggest that the SA_{plot} and LA_{plot} relationship is maintained at larger scales in this particular area and for the five studied species. There is still some variation that is not explained by the models. Thus, it is recommended that allometric characteristics of the trees, such as crown class, soil moisture or even vapor pressure deficit and maximum summer temperature as suggested by [56], could be introduced in the allometry by season, in order to observe what other factors influences SA_{plot}.

Author Contributions: M.R.Q.-P. conducted the lab and field experiments, and together with C.V. conducted the data analysis and wrote the paper.

Funding: This research was funded by the Alberta Ingenuity Fund, NSERC, Consejo Nacional de Ciencia y Tecnología, México, and Universidad Autónoma Metropolitana-Iztapalapa, México.

Acknowledgments: Thanks are due to the Biogeoscience Institute of the University of Calgary, Alberta and field colleague David McAllister. Many thanks to the Reviewers for providing their insightful comments.

Conflicts of Interest: The authors declare no conflict of interest.

References

1. Margolis, H.; Oren, R.; Whitehead, D.; Kaufmann, M.R. Leaf area dynamics of conifer forests. In *Ecophysiology of Coniferous Forests, Physical Ecology*, 1st ed.; Smith, W.K., Hinckley, T.M., Eds.; Academic Press Inc.: San Diego, CA, USA, 1995; pp. 181–223. ISBN 978-0-08-092593-6.
2. Whitehead, D. The estimation of foliage area from sapwood basal area in scots pine. *Forestry* **1978**, *51*, 137–149. [CrossRef]
3. Waring, R. Estimating forest growth and efficiency in relation to canopy leaf area. *Adv. Ecol. Res.* **1983**, *13*, 327–354. [CrossRef]
4. Blanche, C.A.; Hodges, J.D.; Nebeker, T.E. A leaf area-sapwood area ratio developed to rate Loblolly Pine tree vigor. *Can. J. For. Res.* **1985**, *15*, 1181–1184. [CrossRef]
5. Borghetti, M.; Vendramin, G.G.; Giannini, R. Specific leaf area and leaf area index distribution in a young Douglas fir plantation. *Can. J. For. Res.* **1986**, *16*, 1283–1288. [CrossRef]
6. McDowell, N.; Barnard, H.; Bond, B.J.; Hinckley, T.; Hubbard, R.M.; Ishii, H.; K¨ostner, B.; Magnani, F.; Marshall, J.D.; Meinzer, F.C.; et al. The relationships between tree height and leaf area: Sapwood area ratio. *Oecologia* **2002**, *132*, 12–20. [CrossRef] [PubMed]
7. Dean, T.J.; Long, J.N.; Smith, F.W. Bias in leaf area-sapwood area ratios and its impact on growth analysis in *Pinus contorta*. *Trees* **1988**, *2*, 104–109. [CrossRef]
8. Hungerford, R.D. Estimation of foliage area in dense Montana Lodgepole Pine stands. *Can. J. For. Res.* **1987**, *17*, 320–324. [CrossRef]

9. Keane, M.G.; Weetman, G.F. Leaf area-sapwood cross-sectional area relationships in repressed stands of Lodgepole pine. *Can. J. For. Res.* **1987**, *17*, 205–209. [CrossRef]
10. Kaufman, M.R.; Troendle, C. The relationship of leaf area and foliage biomass to sapwood conducting area in four subalpine forest tree species. *For. Sci.* **1981**, *27*, 477–482.
11. Schuler, T.M.; Smith, F.W. Effect of species mix on size/density and leaf-area relations in southwest pinyon/juniper woodlands. *For. Ecol. Manag.* **1988**, *25*, 211–220. [CrossRef]
12. Coyea, M.R.; Margolis, H.A. Factors affecting the relationship between sapwood area and leaf area of Balsam fir. *Can. J. For. Res.* **1992**, *22*, 1684–1693. [CrossRef]
13. Marchand, J.P. Sapwood area as an estimator of foliage biomass and projected leaf area for *Abies balsamea* and *Picea rubens*. *Can. J. For. Res.* **1984**, *14*, 85–87. [CrossRef]
14. Vertessy, R.A.; Benyon, R.G.; O'Sullivan, S.K.; Gribben, P.R. Relationships between stem diameter, sapwood area, leaf area and transpiration in a young mountain ash forest. *Tree Physiol.* **1995**, *15*, 559–567. [CrossRef]
15. Meadows, S.J.; Hodges, D.J. Sapwood area as an estimator of leaf area and foliar weight in Cherrybark oak and green ash. *For. Sci.* **2002**, *48*, 69–76.
16. Binkley, D.; Reid, P. Long-term responses of stem growth and leaf area to thinning and fertilization in a Douglas fir plantation. *Can. J. For. Res.* **1984**, *14*, 656–660. [CrossRef]
17. Shelburne, V.B.; Hedden, R.L.; Allen, R.M. The effects of site, stand density and sapwood permeability on the relationship between leaf area and sapwood area in loblolly pine (*Pinus taeda* L.). *For. Ecol. Manag.* **1993**, *58*, 193–209. [CrossRef]
18. White, D.; Beadle, C.; Worledge, D.; Honeysett, J.; Cherry, M. The influence of drought on the relationship between leaf and conducting sapwood area in *Eucalyptus globulus* and *Eucalyptus nitens*. *Trees* **1998**, *12*, 406–414. [CrossRef]
19. Mencuccini, M.; Grace, J. Climate influences the leaf area/sapwood area ratio in scots pine. *Tree Physiol.* **1994**, *15*, 1–10. [CrossRef]
20. Hillis, W.E. *Heartwood and Tree Exudates*; Series in Wood Science; Springer: Berlin, Germany, 1987; ISBN 3-540-17593-8.
21. Dean, T.J.; Long, J.N. Variation in sapwood area-leaf area relations within two stands of Lodgepole pine. *For. Sci.* **1986**, *32*, 749–758.
22. Lefsky, M.A.; Cohen, W.B.; Acker, S.A.; Parker, G.G.; Spies, T.A.; Harding, D. Lidar remote sensing of the canopy structure and biophysical properties of Douglas fir western hemlock forests. *Remote Sens. Environ.* **1999**, *70*, 339–361. [CrossRef]
23. Means, J.E.; Acker, S.A.; Harding, D.J.; Blair, J.B.; Lefsky, M.A.; Cohen, W.B.; Harmon, M.E.; McKee, W.A. Use of large-footprint scanning airborne LIDAR to estimate forest stand characteristics in the western cascades of Oregon. *Remote Sens. Environ.* **1999**, *67*, 298–308. [CrossRef]
24. Lassen, L.E.; Okkonen, E.A. *Sapwood Thickness of Douglas Fir and Five Other Western Softwoods*; Research Paper FPL-124; US Dept. of Agriculture, Forest Service, Forest Products Laboratory: Madison, WI, USA, 1969; p. 16.
25. Domec, J.C.; Lachenbruch, B.; Pruyn, M.; Spicer, R. Effects of age-related increases on sapwood area, leaf area, and xylem conductivity on height-related hydraulic costs in two contrasting coniferous species. *Ann. For. Sci.* **2012**, *69*, 17–27. [CrossRef]
26. Jaskierniak, D.; Kuczera, G.; Benyon, R.G.; Lucieer, A. Estimating tree and stand sapwood area in spatially heterogeneous southeastern Australian forests. *J. Plant Ecol.* **2016**, *9*, 272–284. [CrossRef]
27. Jaskierniak, D.; Benyon, R.; Kuczera, G.; Robinson, A. A new method for measuring stand sapwood area in forests. *Ecohydrology* **2015**. [CrossRef]
28. Jaskierniak, D.; Kuczera, G.; Benyon, R.; Wallace, L. Using tree detection algorithms to predict sapwood area, basal area and stocking density in *Eucalyptus regnans* forest. *Remote Sens.* **2015**, *7*, 7298–7323. [CrossRef]
29. Mitchell, P.J.; Lane, P.N.J.; Benyon, R.G. Capturing within catchment variation in evapotranspiration from montane forests using LIDAR canopy profiles with measured and modelled fluxes of water. *Ecohydrology* **2012**, *5*, 708–720. [CrossRef]
30. Cˇerm'ak, J.; Nadezhdina, N. Sapwood as the scaling parameter defining according to xylem water content or radial pattern of sap flow? *Ann. Sci. For.* **1998**, *55*, 509–521.
31. Quiñonez-Piñón, M.R.; Valeo, C. Allometry of sapwood depth in five boreal trees. *Forests* **2017**, *8*, 457. [CrossRef]

32. Jonckheere, I.; Fleck, S.; Nackaerts, K.; Muysa, B.; Coppin, P.; Weiss, M.; Baret, F. Review of methods for in situ leaf area index determination. Part I. Theories, sensors and hemispherical photography. *Agric. For. Meteorol.* **2004**, *121*, 19–35. [CrossRef]
33. Peet, R.K. Forests and Meadows of the Rocky Mountains. In *North American Terrestrial Vegetation*, 1st ed.; Barbour, M.G., Billings, W.D., Eds.; Cambridge University Press: New York, NY, USA, 1988; ISBN 13-978-0-52-126198-2.
34. Rowe, J.S. *Forest Regions of Canada*; Department of the Environment Canadian Forestry Service: Ottawa, ON, Canada, 1972; p. 177.
35. Strong, W.L.; Leggat, K.R. Ecoregions of Alberta. In *Forestry, Lands, and Wildlife (1986–1993)*; The Provincial Archives of Alberta: Edmonton, AB, Canada, 1992; p. 59.
36. Elliot-Frisk, D.L. The taiga and boreal forest. In *North American Terrestrial Vegetation*, 1st ed.; Barbour, M.G., Billings, W.D., Eds.; Cambridge University Press: New York, NY, USA, 1988; ISBN 13-978-0-52-126198-2.
37. Quiñonez-Piñón, M.R.; Valeo, C. Assessing the translucence and color-change methods for estimating sapwood depth in three boreal species. *Forests* **2018**, *9*, 686. [CrossRef]
38. Kramer, P.J.; Kozlowski, T.T. *Physiology of Woody Plants*, 1st ed.; Academic Press Inc.: New York, NY, USA, 1979.
39. Payton, M.E.; Miller, A.E.; Raun, W.R. Testing statistical hypothesis using standard error bars and confidence intervals. *Commun. Soil Sci. Plant Anal.* **2000**, *31*, 547–551. [CrossRef]
40. Vangel, M.G. Confidence intervals for a normal coefficient of variation. *Am. Stat.* **1996**, *50*, 21–26.
41. Verrill, S. *Confidence Bounds for Normal and Log Normal Distribution Coefficients of Variation*; Research Paper FPL-RP-609; The Forest Products Laboratory: Madison, WI, USA, 2003; pp. 1–10.
42. Payton, M.E. Confidence intervals for the coefficient of variation. In *Refereed Proceedings for the 1996 Kansas State University Conference for Applied Statistics in Agriculture*; Kansas State University: Manhattan, KS, USA, 1997; pp. 82–87.
43. Chen, J.M.; Cihlar, J. Retrieving leaf area index of boreal conifer forests using Landsat-TM Images. *Remote Sens. Environ.* **1996**, *55*, 153–162. [CrossRef]
44. Leblanc, S.G.; Chen, J.M.; Kwong, M. *Tracing Radiation and Architecture of Canopies. TRAC Manual Version 2.1.3.*, 1st ed.; Natural Resources Canada, Canada Centre for Remote Sensing: Ottawa, ON, Canada, 2002.
45. Chen, J.M.; Rich, P.M.; Gower, S.T.; Norman, J.M.; Plummer, S. Leaf area index of boreal forests: Theory, techniques, and measurements. *J. Geophys. Res.* **1997**, *102*, 429–443. [CrossRef]
46. Robinson, D.E.; Wagner, R.G.; Swanton, C.J. Effects of nitrogen on the growth of Jack pine competing with Canada blue-joint grass and large leaved aster. *For. Ecol. Manag.* **2002**, *160*, 233–242. [CrossRef]
47. Chapra, S.C.; Canale, R.P. *Numerical Methods for Engineers*, 2nd ed.; McGraw Hill, Inc.: New York, NY, USA, 1988; p. 833. ISBN 13-9780079099440.
48. Sperry, J.; Tyree, M.T. Water-stress-induced xylem embolism in three species of conifers. *Plant Cell Environ.* **1989**, *13*, 427–436. [CrossRef]
49. Xiao, C.W.; Janssens, J.; Curiel, Y.; Ceulemans, R. Variation of specific leaf area and upscaling to leaf area index in mature Scots pine. *Trees* **2006**, *20*, 304. [CrossRef]
50. Scheinder, R.; Berninger, F.; Ung, C.; Bernier, P.Y.; Swift, D.E.; Zhang, S.Y. Calibration of jack pine allometric relationships with simultaneous regressions. *Can. J. For. Res.* **2008**, *38*, 2566. [CrossRef]
51. Thurner, M.; Beer, C.; Crowther, T.; Falster, D.; Manzoni, S.; Prokushkin, A.; Schulze, E.D. Supporting Information for Sapwood Biomass Carbon in Northern Boreal and Temperate Forests. 2019. Available online: https://pure.mpg.de\T1\guilsinglrightitem_3065977_1\T1\guilsinglrightcomponent\T1\guilsinglrightfile_3065979\T1\guilsinglrightcontent (accessed on 16 August 2019).
52. Shinohara, Y.; Komatsu, H.; Otsuki, K. Sapwood and intermediate wood variations in Japanese cedar: Impacts on sapwood area estimates. *Hydrol. Res. Lett.* **2015**, *9*, 35. [CrossRef]
53. Quinn, G.P.; Keough, M.J. *Experimental Design and Data Analysis for Biologists*, 1st ed.; Cambridge University Press: Cambridge, UK, 2002.
54. Hernandez-Santana, V.; Hernandez-Hernandez, A.; Vadenboncoeur, M.A.; Asbjornsen, H. Scaling from single-point sap velocity measurements to stand transpiration in a multispecies deciduous forest: Uncertainty sources, stand structure effect, and future scenarios. *Can. J. For. Res.* **2015**, *45*, 1489. [CrossRef]

55. Bell, D.M.; Ward, E.J.; Oishi, C.; Oren, R.; Flikkema, P.G.; Clark, J.S. A state-space modeling approach to estimating the canopy conductance and associated uncertainties from sap flux density data. *Tree Physiol.* **2015**, *35*, 792–802. [CrossRef]
56. Mencuccini, M.; Bonosi, L. Leaf/sapwood area ratios in Scots pine show acclimation across Europe. *Can. J. For. Res.* **2001**, *31*, 442. [CrossRef]